

Effects of Processing Conditions on Nanoclay Dispersion in Starch-Clay Nanocomposites

Bor-Sen Chiou,^{1,2} Emma Yee,¹ Delilah Wood,¹ Justin Shey,¹ Greg Glenn,¹ and William Orts¹

ABSTRACT

Cereal Chem. 83(3):300–305

Wheat starch samples containing Cloisite Na+ and 30B nanoclays were extruded from a twin-screw extruder. Moisture content, temperature, and screw speed were varied to determine their effect on nanoclay dispersion. X-ray diffraction and transmission electron microscopy (TEM) were used to examine nanoclay intercalation and exfoliation. Moisture content had the largest effect on Cloisite Na+ dispersion, with the highest moisture sample containing exfoliated nanoclays. Meanwhile, temperature and

screw speed had little effect on Cloisite Na+ dispersion. For Cloisite 30B samples, only an increase in temperature produced slight intercalation of nanoclays. This was due to the incompatibility of starch with the more hydrophobic Cloisite 30B. Also, Cloisite Na+ and 30B intercalation did not depend on specific mechanical energy. In addition, water absorbance tests indicated the Cloisite Na+ sample containing the most well-dispersed nanoclays had the lowest water uptake.

One promising method of producing nanoclay composites involves melt intercalation, where polymer chains diffuse into the interlayer between clay platelets. This approach allows nanocomposites to be produced by using conventional polymer melt compounding equipment such as extruders. This is simpler and more economical than other techniques such as intercalation through in situ polymerization of intercalated monomers or intercalation from solution. Studies on using extruders to form nanoclay composites had only appeared within the last few years (Cho et al 2001; Dennis et al 2001; Fornes et al 2001, 2004; Nam et al 2001; Wang et al 2001; Krook et al 2002; Maiti et al 2002; Ray et al 2002, 2003; Incarnato et al 2003, 2004; Yoon et al 2003; Zhu et al 2004). These studies mainly involved synthetic polymers derived from petroleum such as nylon 6 (Cho et al 2001; Fornes et al 2001, 2004; Wang et al 2001), polypropylene (Nam et al 2001; Wang et al 2001; Maiti et al 2002; Zhu et al 2004), polyamides (Dennis et al 2001; Krook et al 2002; Incarnato et al 2003; Incarnato et al 2004), polycarbonate (Yoon et al 2003), and polystyrene (Wang et al 2001).

There have been very few studies on nanoclay composites containing natural polymers. In one study, Park et al (2002, 2003) mixed potato starch with various nanoclays in a mixer. They found that incorporating nanoclay resulted in materials with higher tensile strength, reduced water vapor transmission, and improved thermal stability. Xu et al (2005) extruded starch acetate/nanoclay foams and determined that the foams had reduced compressibility and improved thermal stability. Another study by McGlashan et al (2003) examined blown films involving low-amylose wheat starch and chemically modified high-amylose maize starch with nanoclay and an aliphatic polyester. Park et al (2004a,b) also studied nanoclay composites containing cellulose acetates. In addition, Kalambur et al (2005) incorporated nanoclays into wheat starch/polycaprolactone blends. These studies (McGlashan et al 2003, Park et al 2004a,b; Kalambur et al 2005) showed that adding nanoclay increased the modulus and strength of the materials.

Most studies on extrusion of nanoclay composites had focused on their final material properties. Only a few studies included the effects of processing conditions on nanoclay intercalation. In one

study, Dennis et al (2001) used several types of extruders and screw configurations to produce polyamide/nanoclay composites. The authors found that twin-screw extruders provided better nanoclay dispersion than a single-screw extruder. For each twin-screw extruder, medium levels of shear gave the best clay dispersion. A longer mean residence time also improved clay dispersion. In another study, Cho et al (2001) also determined that a twin-screw extruder dispersed clays better than a single-screw extruder for a nylon 6/nanoclay composite. Others (Krook et al 2002; Incarnato et al 2003, 2004) had examined the effects of screw speed on nanoclay dispersion. Krook et al (2002) found that an increase in screw speed produced polyesteramide/nanoclay samples with lower X-ray peak intensities. This indicated that increased shear might have exfoliated some of the nanoclays. In addition, Incarnato et al (2003, 2004) determined that polyamide/nanoclay samples extruded at higher screw speeds had greater elastic modulus and complex viscosity values. They attributed these results to better nanoclay dispersion from greater shear at high screw speeds.

In this study, we examined the effects of processing conditions on nanoclay dispersion in wheat starch/nanoclay composites. We used a co-rotating twin-screw extruder and varied moisture content, screw speed, and extrusion temperature. We studied two different nanoclays, Cloisite Na+, which has a hydrophilic interlayer, and Cloisite 30B, which has a more hydrophobic interlayer. We examined Cloisite 30B because it is the closest nanoclay to Cloisite Na+ in terms of hydrophilicity. We used X-ray diffraction and transmission electron microscopy (TEM) to characterize nanoclay dispersion. In addition, we measured the water absorbance of the samples.

MATERIALS AND METHODS

Materials

Wheat starch and two types of nanoclays were used in this study. Wheat starch was Midsol 50 from Midwest Grain Products and contained 12.5 wt% moisture. The nanoclays were Cloisite Na+ and Cloisite 30B from Southern Clay Products. Cloisite Na+ is unmodified and is more hydrophilic than Cloisite 30B, which is modified with methyl, tallow, bis-2-hydroxyethyl, quaternary ammonium. A concentration of 5 wt% nanoclay was used for all extrusion experiments. This concentration was chosen because a previous study (Park et al 2003) indicated 5 wt% nanoclay in potato starch resulted in composites with the best material properties.

Extrusion

A Leistritz Micro 18 co-rotating twin-screw extruder was used to prepare the starch-nanoclay composites. The extruder has six heating zones with the first five cooled by water. The screws have

¹ Bioproduct Chemistry and Engineering, U.S. Department of Agriculture, ARS, WRR, 800 Buchanan Street, Albany, CA 94710. Names are necessary to report factually on available data; however, the USDA neither guarantees nor warrants the standard of the product, and the use of the name by the USDA implies no approval of the product to the exclusion of others that may also be suitable.

² Corresponding author: Phone: 510-559-5628. Fax: 510-559-5675. E-mail: bschiou@pw.usda.gov

a diameter of 18 mm and the barrel has a length to diameter ratio of 30:1. The configuration and type of screw elements used in the experiments are shown in Table I. A K-Tron Soder T-20 loss-in-weight feeder was used to control the solids (starch and clay powder) feed rate. A Bran + Luebbe N-P31 metering pump was used to control the deionized water feed rate.

Three different processing variables were adjusted to determine their effects on intercalation and exfoliation of nanoclay during extrusion. The first involved the solid to liquid ratio, which was maintained at 1.5, 2, and 3:1. These solid to liquid ratios corresponded to samples with moisture contents of 47, 41, and 34 wt%, respectively. The solid feed rate was kept constant at 12 g/min and the water feed rate was varied to produce the requisite ratios. Each sample is designated as nanoclay/percent moisture. For instance, a Cloisite Na+ sample with 34 wt% moisture is named Cloisite Na+/34. The second variable was screw speed, which was set at 30, 60, 120, and 180 rpm. The third variable was barrel temperature, which varied from 100 to 130°C. The complete temperature profiles for the various runs are shown in Table II. The product temperature was close to the barrel temperature measured in zone 6. For simplicity, the highest temperature reached during each run is used to designate that temperature profile.

The specific mechanical energy (SME) is the amount of mechanical energy dissipated as heat inside the material during the extrusion process. The SME can be determined by using

$$SME = sP\tau/100s_m m_f \quad (1)$$

where s is the screw speed, P is the power (2200 J/sec), τ is the percent torque, s_m is the maximum screw speed (500 rpm), and m_f is the total mass feed rate.

X-ray Diffraction

Nanoclay d_{001} spacings were measured by wide-angle X-ray diffraction using a Philips X'Pert MPD X-ray diffractometer. The samples were prepared by first cryogrinding them using a Mikro-Bantam model SH mill (Hosokawa Micron Powder Systems). The powder was then sieved using a 270 mesh (53 μ m) sieve. $\text{CuK}\alpha_1$ radiation with a wavelength of 0.154 nm was used in the experiments and the radiation was generated at 45kV and 40mA. The samples were scanned at a speed of 0.03°/sec. The d_{001} spacing was calculated by first determining 2θ for the scattering peak

using the Phillips X'Pert Data Viewer software and then substituting the 2θ value into Bragg's Law.

Transmission Electron Microscopy (TEM)

An RMC Powertome-X untramicrotome equipped with the CR-X Cryosectioning System (Boeckeler Instruments, Tucson, AZ) was used to section the starch-nanoclay samples. The sample was mounted using a pinch-clamp specimen mount and placed directly onto a chuck in the chilled ultramicrotome chamber. The sample was sectioned into pieces 80–90 nm thick at temperatures of -70 to -75°C . Sections were viewed and photographed using a Philips CM-12 transmission electron microscope.

Water Absorbance

The water absorbance of the nanoclay samples was determined according to ASTM D570-98. The samples were first conditioned for one week in 50% relative humidity at 23°C . The samples were exposed to these conditions after they were placed in a chamber containing a saturated solution of calcium nitrate tetrahydrate, $\text{Ca}(\text{NO}_3)_2 \cdot 4\text{H}_2\text{O}$ (Fisher), in deionized water. All samples were 7 cm long and 4 mm in diameter. After the conditioning period, the samples were dried at 50°C for 24 hr. Each sample was soaked in deionized water for 2, 4, 6, 8, and 24 hr, after which it was blotted dry with paper towels and weighed. The weight change was determined for each sample. For samples containing nanoclay, their weight change was normalized by dividing by the weight change of neat starch samples containing the same moisture content during extrusion. This normalized value is determined by using

$$W(t) = \frac{(w_n(t) - w_n(0))/w_n(0)}{(w_s(t) - w_s(0))/w_s(0)} \quad (2)$$

where $W(t)$ is the normalized weight change at time t , $w_n(t)$ is the weight of the nanoclay sample at time t , $w_n(0)$ is the weight of the nanoclay sample before soaking, $w_s(t)$ is the weight of the neat starch sample at time t , and $w_s(0)$ is the weight of the neat starch sample before soaking.

RESULTS AND DISCUSSION

Nanoclay Dispersion in Composites

We first examined the effects of moisture content on nanoclay dispersion in extruded starch-nanoclay composites. X-ray diffraction results indicated the Cloisite Na+/47 sample contained exfoliated nanoclay, whereas the Cloisite Na+/34 and Cloisite Na+/41

TABLE I
Screw Configuration

Type of Element ^a	Pitch (cm)	Overall Length (cm)	Kneading Blocks	Angle (°)
Conveying ^b	3	9	–	–
Conveying	2	9	–	–
Kneading block	–	2	4	30
Kneading block	–	2	4	60
Conveying	1	9	–	–
Kneading block	–	2	4	90
Kneading block	–	2	4	90
Conveying	2	12	–	–
Conveying	1	6	–	–

^a All elements are double-flighted.

^b Screw element descriptions proceed from feed end to die end.

TABLE II
Temperature Profiles in Extruder

Temp. (°C)	Zones					
	1	2	3	4	5	6
100	80	100	100	100	100	100
110	80	100	110	100	110	100
120	80	100	120	110	120	115
130	80	105	130	115	130	125

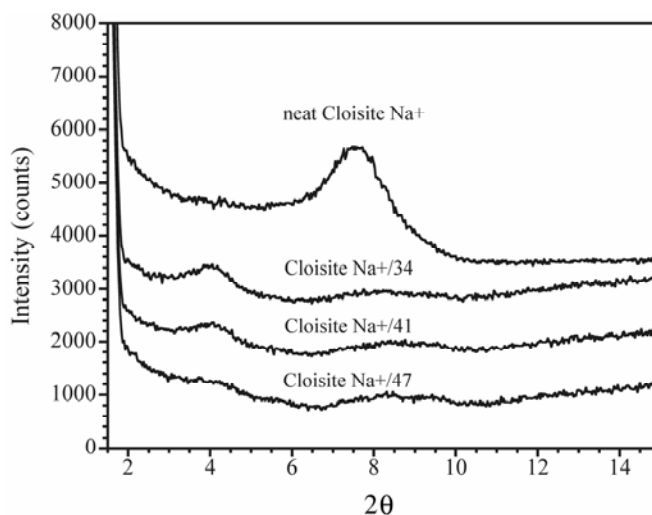


Fig. 1. X-ray diffraction data for Cloisite Na+ samples extruded at various moisture contents. Temperature 100°C and screw speed 30 rpm. Each curve was shifted by 1,000 counts from the adjacent curve.

samples contained intercalated nanoclay. This is shown in Fig. 1, where we plot the diffraction data of extruded 5 wt% Cloisite Na+ samples with different moisture contents as a function of 2θ . The temperature was 100°C and screw speed was 30 rpm. The diffraction result for neat Cloisite Na+ nanoclay is also shown in Fig. 1. The Cloisite Na+/47 sample showed almost no diffraction peak. In contrast, the Cloisite Na+/34 and Cloisite Na+/41 samples had 2θ peaks at 4.06° and 4.04°, respectively, which corresponded to d_{001} spacings of 2.17 and 2.19 nm. As a comparison, neat Cloisite Na+ has a d_{001} spacing of 1.17 nm. These results might be explained by the swelling of Cloisite Na+ by water. An increase in water content leads to more swelling and eventual exfoliation of the nanoclay. The results might also be explained by the greater degree of gelatinization at higher moisture contents. Greater gelatinization means more disruption of starch granule structure and more leaching of amylose and amylopectin from the granule. Both amylose and amylopectin contain hydroxy groups, rendering them hydrophilic. These molecules can then penetrate into the Cloisite Na+ interlayer. At higher moisture contents, there should be a greater amount of amylose and amylopectin available for interlayer penetration. More interpenetration leads to greater interlayer spacing, consistent with the results shown in Fig. 1.

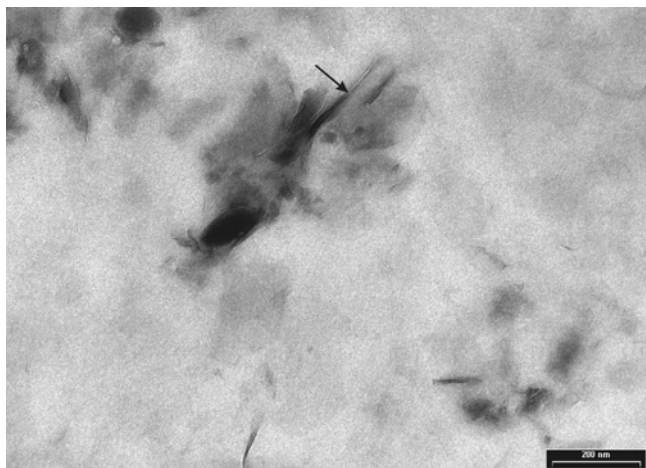


Fig. 2. Transmission electron micrograph (TEM) of Cloisite Na+/47 sample. Arrow indicates nondispersed nanoclay platelets.

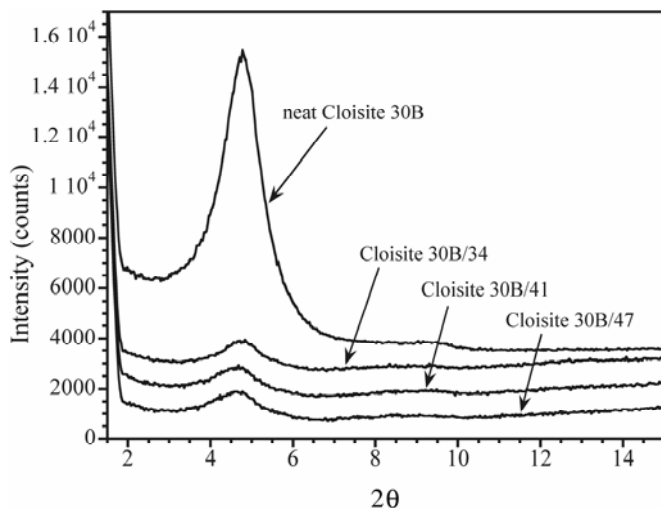


Fig. 3. X-ray diffraction data for Cloisite 30B samples extruded at various moisture contents. Temperature 100°C and screw speed 30 rpm. Each curve was shifted by 1,000 counts from the adjacent curve.

Although the Cloisite Na+/47 sample displayed almost no nanoclay diffraction peak, the sample did contain nanoclay particles that did not fully exfoliate. This is shown in a TEM micrograph in Fig. 2, which shows clusters of Cloisite Na+ nanoclay that did not evenly disperse in the sample. These clusters contained individual platelets that still retained their stacked structure. The presence of these stacked structures indicated that the sample contained a mixture of intercalated and exfoliated nanoclays.

When we varied the moisture content for samples containing Cloisite 30B, we obtained very different results than those from Cloisite Na+ samples. X-ray diffraction results indicated that nanoclay intercalation did not occur in the Cloisite 30B samples. This is shown in Fig. 3, where we plot the diffraction data for extruded 5 wt% Cloisite 30B samples with different moisture contents as a function of 2θ . The temperature was 100°C and the screw speed was 30 rpm. The diffraction result for the neat Cloisite 30B nanoclay is also included in Fig. 3. The three samples had practically the same 2θ peak value as neat Cloisite 30B clay, indicating moisture level during extrusion did not affect the interlayer spacings. Cloisite 30B is more hydrophobic than Cloisite Na+, making it more difficult for water, amylose, and amylopectin to penetrate the Cloisite 30B interlayer. The authors in previous studies (Park et al 2002, 2003) found a slight shift in 2θ peak value after compounding potato starch and Cloisite 30B in a mixer.

We next varied screw speed and temperature for the Cloisite Na+/47 samples. However, all X-ray diffraction results for these samples displayed very small or no diffraction peaks, similar to that shown in Fig. 1. Consequently, we decided to focus on Cloisite Na+/34 samples, which showed a distinct diffraction peak, to determine the effects of processing conditions on nanoclay dispersion. We first varied screw speed and kept the extruder temperature at 100°C. All Cloisite Na+ samples had comparable 2θ peak values and showed nanoclay intercalation. This is shown in Fig. 4, where we plot the diffraction data for 5 wt% Cloisite Na+ samples extruded at different screw speeds as a function of 2θ . These results indicated that screw speed did not have much effect on Cloisite Na+ dispersion.

We also examined the effects of screw speed on nanoclay dispersion in Cloisite 30B/34 samples. Screw speed had virtually no effect on Cloisite 30B dispersion. This is shown in Fig. 5, where we plot 5 wt% Cloisite 30B samples extruded at different screw speeds as a function of 2θ . The temperature was 100°C. All samples had comparable 2θ peak values, indicating screw speed had little effect on nanoclay interlayer spacing.

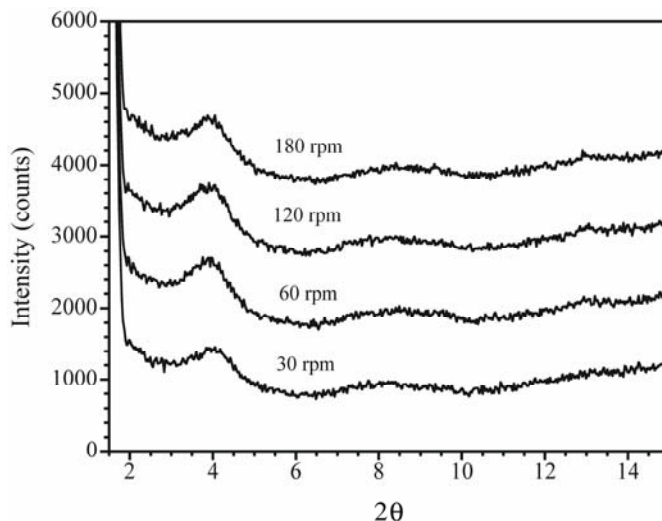


Fig. 4. X-ray diffraction data for Cloisite Na+/34 samples extruded at various screw speeds. Temperature 100°C. Each curve was shifted by 1,000 counts from the adjacent curve.

Previous studies examining the effects of shear on nanoclay dispersion reached different conclusions. Some authors determined shear to be a factor in clay dispersion (Dennis et al 2001; Krook et al 2002; Incarnato et al 2003, 2004; Zhu et al 2004), whereas others found that different levels of shear had little effect on clay dispersion (Lim et al 2000; Riva et al 2002). In one study, Dennis et al (2001) determined that medium shear in twin-screw extruders proved most effective in dispersing clay for a polyamide/nanoclay system. Meanwhile, Krook et al (2002) found a decrease in X-ray intensity in three of four polyesteramide/nanoclay samples after increasing screw speed from 30 to 60 rpm in a twin-screw extruder. They attributed these results to greater shear rates at higher screw speeds, which provided better clay dispersion. Similarly, Incarnato et al (2003, 2004) used a twin-screw extruder to produce polyamide/nanoclay samples and determined that an increase in screw speed from 50 to 100 rpm resulted in samples with better clay dispersion (Incarnato et al 2003). In contrast, Riva et al (2002) showed that processing a poly(ethylene-co-vinylacetate)/nanoclay composite with a mixer and twin-screw extruder resulted in samples with the same X-ray diffraction pattern. Also, Lim et al (2000) found that a polystyrene/nanoclay composite produced in a mixer, under high shear, and a rheometer, under low shear, had comparable peak 2θ values.

Our extrusion results and those from other studies on different polymer/nanoclay systems indicated that polymer-nanoclay compatibility had a greater effect on nanoclay dispersion than shear. There are three general classes of nanoclay systems (Dennis et al 2001). The first involves clay and polymer systems that are compatible with each other. In this case, any type of processing results in clay exfoliation. The second class involves clay and polymer systems that are marginally compatible. For this system, processing conditions need to be optimized to produce exfoliated nanoclays. The third class involves clay and polymer systems that are not compatible. In this case, the processing conditions need to be optimized to obtain intercalated clays, but exfoliation may not be possible. From our results, wheat starch is compatible with Cloisite Na+ once sufficient moisture is present during extrusion. On the other hand, wheat starch is not compatible with Cloisite 30B because no exfoliation occurred under any processing conditions in this study.

We next examined the effects of extruder temperature on nanoclay dispersion in 34 wt% moisture samples. Temperature did not have much effect on Cloisite Na+ clay intercalation. This is shown in Fig. 6, where we plot the diffraction data for 5 wt% Cloisite Na+ samples extruded at various temperatures as a function of 2θ .

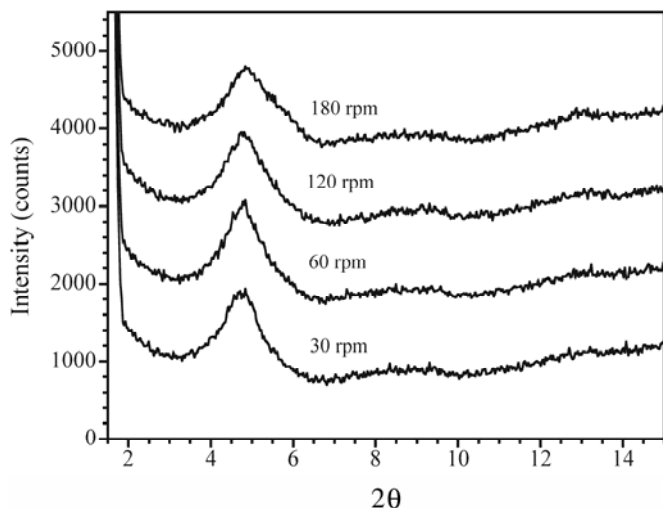


Fig. 5. X-ray diffraction data for Cloisite 30B/34 samples extruded at various screw speeds. Temperature 100°C. Each curve was shifted by 1,000 counts from the adjacent curve.

The screw speed was 30 rpm. An increase in temperature leads to a greater degree of gelatinization. Samples extruded at higher temperatures should contain greater amounts of amylose and amylopectin available for interlayer penetration. However, all samples had comparable 2θ values over the temperature range. This indicated that nanoclay intercalation was not affected by the different degrees of gelatinization at the temperatures reached during extrusion.

When we increased extrusion temperature for Cloisite 30B/34 samples, the nanoclay became slightly intercalated. This is shown in Fig. 7, where we plot the X-ray diffraction data for 5 wt% Cloisite 30B samples extruded at different temperatures as a function of 2θ . The screw speed was 30 rpm. The d_{001} spacing increased from 1.85 nm at 100°C to 2.09 nm at 130°C. This behavior differed from that of the Cloisite Na+ samples, where the d_{001} spacings did not change at higher temperatures. Authors from previous studies (Vaia et al 1994, 1997) also found little or no change in d_{001} spacings for samples containing modified nanoclays heated to higher temperatures. However, Di et al (2003) determined that a polycaprolactone/nanoclay sample blended at 180°C had an X-ray diffraction peak, whereas the sample blended at 100°C did not have any peak. They attributed this result to the lower tem-

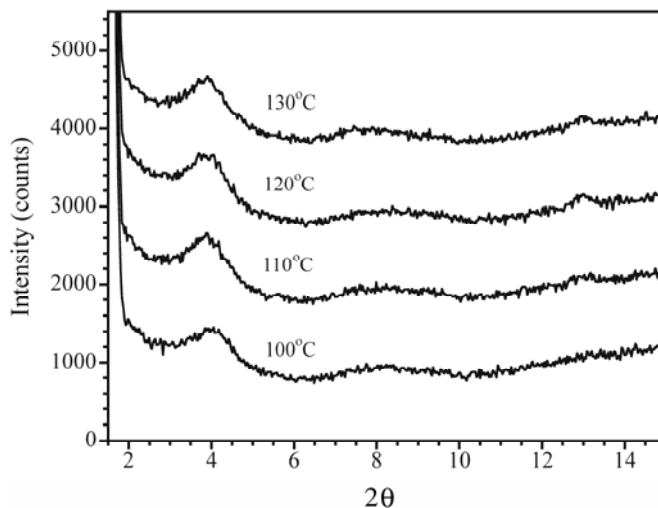


Fig. 6. X-ray diffraction data for Cloisite Na+/34 samples extruded at various temperatures. Screw speed 30 rpm. Each curve was shifted by 1,000 counts from the adjacent curve.

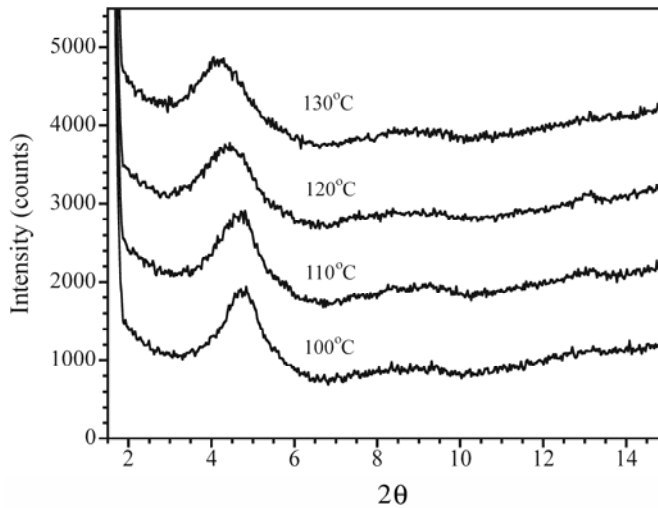


Fig. 7. X-ray diffraction data for Cloisite 30B/34 samples extruded at various temperatures. Screw speed 30 rpm. Each curve was shifted by 1,000 counts from the adjacent curve.

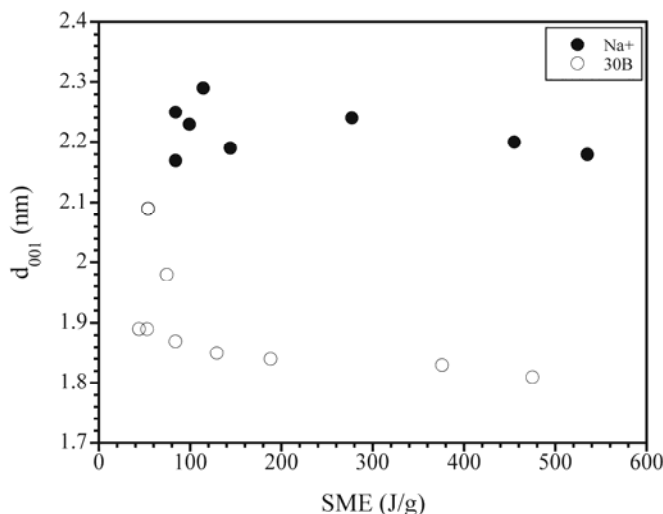


Fig. 8. The d_{001} spacings of nanoclay samples as a function of specific mechanical energy.

perature sample having a higher viscosity, leading to greater shear stress and better clay dispersion.

We calculated specific mechanical energies for the Cloisite Na+ and 30B samples and found it had no effect on d_{001} spacings. This is shown in Fig. 8, where we plot the d_{001} spacings for the Cloisite Na+ and 30B samples as a function of specific mechanical energy. During extrusion, high shear and temperature cause starch molecules to break down and form lower molecular weight species. One parameter that has been shown to correlate with molecular breakdown is specific mechanical energy. Previous studies had shown that starch samples that experienced higher specific mechanical energies formed molecules with lower molecular weights (Willett et al 1997; Brummer et al 2002). The decrease in molecular weight resulted in samples with lower intrinsic viscosity (Della Valle et al 1995; Martin et al 2003), lower melt viscosity (Della Valle et al 1995; Chang et al 1999; Martin et al 2003), and higher water solubility index (Kirby et al 1988). The results for Cloisite 30B samples make sense because starch molecules should have difficulty penetrating the Cloisite 30B interlayer, no matter the molecular weight. The Cloisite Na+ intercalation process is also not affected by changes in starch molecular weight.

Water Absorbance

Although this study mainly focused on the effects of processing conditions on nanoclay dispersion, we also examined water absorbance of the extruded samples. The Cloisite Na+/47 sample proved most effective in limiting water uptake. The results are shown in Fig. 9, where we plot the normalized weight change of nanoclay samples as a function of time. The Cloisite Na+/47 sample had $\approx 50\text{--}60\%$ of the weight gain of neat starch. In contrast, the Cloisite Na+/34 sample had comparable weight increases to the neat starch sample. Meanwhile, the Cloisite 30B/34 sample had $\approx 80\text{--}90\%$ of the weight gain of neat starch. These results can be explained by examining nanoclay dispersion and nanoclay hydrophobicity. The Cloisite Na+/47 sample contained exfoliated nanoclays, whereas the Cloisite Na+/34 sample contained intercalated nanoclays. Consequently, water molecules take a more tortuous path through the Cloisite Na+/47 sample, resulting in slower water uptake compared with the others. The Cloisite 30B/34 sample is more effective than the Cloisite Na+/34 sample in preventing water uptake because Cloisite 30B is more hydrophobic than Cloisite Na+. In this case, clay dispersion did not make much difference because the Cloisite Na+/34 sample contained intercalated clays, whereas the Cloisite 30B/34 sample showed no intercalation.

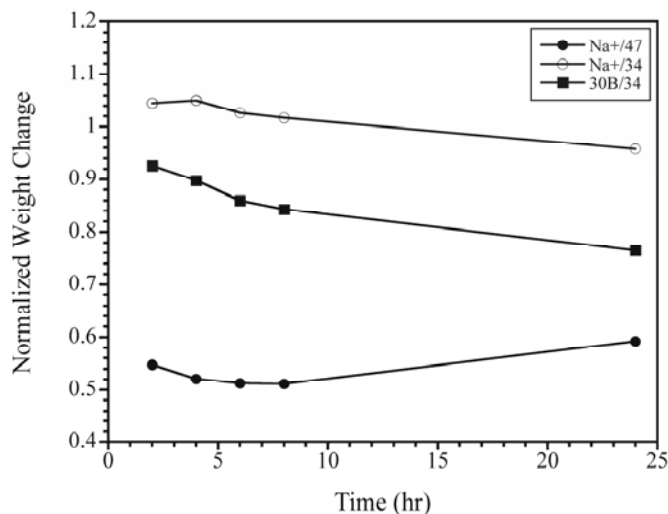


Fig. 9. Normalized water absorbance for nanoclay samples as a function of time. Lines are drawn only as a guide.

CONCLUSIONS

We examined the effects of moisture content, temperature, and screw speed on nanoclay dispersion in extruded wheat starch samples. Moisture content was the major factor affecting Cloisite Na+ dispersion. Cloisite Na+ samples with 47 wt% moisture during extrusion contained exfoliated nanoclays, whereas Cloisite Na+ samples with lower moisture content contained intercalated nanoclays. Other processing parameters, such as extrusion temperature and screw speed, had little effect on Cloisite Na+ dispersion. For the Cloisite 30B samples, only an increase in temperature resulted in slight intercalation of nanoclay. A change in moisture content and screw speed did not produce intercalation. This was due to starch being incompatible with the more hydrophobic Cloisite 30B interlayer. Specific mechanical energy also did not have an effect on interlayer spacing for both Cloisite Na+ and 30B samples.

Nanoclay dispersion and hydrophobicity affected water uptake in the nanoclay composites. The Cloisite Na+ sample with exfoliated nanoclay absorbed less water than the Cloisite Na+ sample with intercalated nanoclay. This might be due to better dispersed clays providing a more effective barrier to water molecules. The Cloisite 30B sample also absorbed less water than the Cloisite Na+ sample containing intercalated clay. This might be due to Cloisite 30B being more hydrophobic than Cloisite Na+.

ACKNOWLEDGMENTS

We acknowledge Michael Dunlap for use of the Philips CM12 TEM at University of California Davis and Robert Chioveti of Boeckeler Instruments for presenting the workshop, which allowed us to collect the cryo sections.

LITERATURE CITED

- Brummer, T., Meusser, F., van Lengerich, H., and Niemann, C. 2002. Effect of extrusion cooking on molecular parameters of corn starch. *Starch* 54:1-8.
- Chang, Y. K., Martinez-Bustos, F., Park, T. S., and Kokini, J. L. 1999. The influence of specific mechanical energy on commel viscosity measured by an on-line system during twin-screw extrusion. *Brazilian J. Chem. Eng.* 16: 285-295.
- Cho, J. W., and Paul, D. R. 2001. Nylon 6 nanocomposites by melt compounding. *Polymer* 42:1083-1094.
- Della Valle, G., Boche, Y., Colonna, P., and Vergnes, B. 1995. The extrusion behavior of potato starch. *Carbohydr. Polym.* 28:255-264.
- Dennis, H. R., Hunter, D. L., Chang, D., Kim, S., White, J. L., Cho, J. W., and Paul, D. R. 2001. Effect of melt processing conditions on the

- extent of exfoliation in organoclay-based nanocomposites. *Polymer* 42: 9513-9522.
- Di, Y., Iannace, S., Di Maio, E., and Nicolais, L. 2003. Nanocomposites by melt intercalation based on polycaprolactone and organoclay. *J. Polym. Sci.: Part B: Polym. Phys.* 41:670-678.
- Fornes, T. D., Yoon, P. J., Keskkula, H., and Paul, D. R. 2001. Nylon 6 nanocomposites: The effect of matrix molecular weight. *Polymer* 42:9929-9940.
- Fornes, T. D., Hunter, D. L., and Paul, D. R. 2004. Nylon-6 nanocomposites from alkylammonium-modified clay: The role of alkyl tails on exfoliation. *Macromolecules* 37:1793-1798.
- Incarnato, L., Scarfata, P., Russo, G. M., Di Maio, L., Iannelli, P., and Acierno, D. 2003. Preparation and characterization of new melt compounded copolyamide nanocomposites. *Polymer* 44:4625-4634.
- Incarnato, L., Scarfata, P., Scatteia, L., and Acierno, D. 2004. Rheological behavior of new melt compounded copolyamide nanocomposites. *Polymer* 45:3487-3496.
- Kalambur, S., and Rizvi, S. S. H. 2005. Biodegradable and functionally superior starch-polyester nanocomposites from reactive extrusion. *J. Appl. Polym. Sci.* 96:1072-1082.
- Kirby, A. R., Ollett, A.-L., Parker, R., and Smith, A. C. 1988. An experimental study of screw configuration effects in the twin-screw extrusion-cooking of maize grits. *J. Food Eng.* 8:247-272.
- Krook, M., Albertsson, A.-C., Gedde, U. W., and Hedenqvist, M. S. 2002. Barrier and mechanical properties of montmorillonite/polyesteramide nanocomposites. *Polym. Eng. Sci.* 42:1238-1246.
- Lim, Y. T., and Park, O. O. 2000. Rheological evidence for the microstructure of intercalated polymer/layered silicate nanocomposites. *Macromol. Rapid Commun.* 21:231-235.
- Maiti, P., Nam, P. H., Okamoto, M., Hasegawa, N., and Usuki, A. 2002. Influence of crystallization on intercalation, morphology, and mechanical properties of polypropylene/clay nanocomposites. *Macromolecules* 35:2042-2049.
- Martin, O., Averous, L., and Della Valle, G. 2003. In-line determination of plasticized wheat starch viscoelastic behavior: Impact of processing. *Carbohydr. Polym.* 53:169-182.
- McGlashan, S. A., and Halley, P. J. 2003. Preparation and characterization of biodegradable starch-based nanocomposite materials. *Polym. Int.* 52:1767-1773.
- Nam, P. H., Maiti, P., Okamoto, M., Kotaka, T., Hasegawa, N., and Usuki, A. 2001. A hierarchical structure and properties of intercalated polypropylene/clay nanocomposites. *Polymer* 42:9633-9640.
- Park, H.-M., Li, X., Jin, C. Z., Park, C. Y., Cho, W. J., and Ha, C.-S. 2002. Preparation and properties of biodegradable thermoplastic starch/clay hybrids. *Macromol. Mater. Eng.* 287:553-558.
- Park, H.-M., Lee, W.-K., Park, C.-Y., Cho, W.-J., and Ha, C.-S. 2003. Environmentally friendly polymer hybrids. 1. Mechanical, thermal, and barrier properties of thermoplastic starch/clay nanocomposites. *J. Mater. Sci.* 38:909-915.
- Park, H.-M., Liang, X., Mohanty, A. K., Misra, M., and Drzal, L.T. 2004a. Effect of compatibilizer on nanostructure of the biodegradable cellulose acetate/organoclay nanocomposites. *Macromolecules* 37:9076-9082.
- Park, H.-M., Misra, M., Drzal, L. T., and Mohanty, A. K. 2004b. Green nanocomposites from cellulose acetate bioplastic and clay: Effect of eco-friendly triethyl citrate plasticizer. *Biomacromolecules* 5:2281-2288.
- Ray, S. S., Maiti, P., Okamoto, M., Yamada, K., and Ueda, K. 2002. New polylactide/layered silicate nanocomposites. 1. Preparation, characterization, and properties. *Macromolecules* 35:3104-3110.
- Ray, S. S., Okamoto, K., and Okamoto, M. 2003. Structure-property relationship in biodegradable poly(butylene succinate)/layered silicate nanocomposites. *Macromolecules* 36:2355-2367.
- Riva, A., Zanetti, M., Braglia, M., Camino, G., and Falqui, L. 2002. Thermal degradation and rheological behaviour of EVA/montmorillonite nanocomposites. *Polym. Degr. Stab.* 77:299-304.
- Vaia, R. A., and Giannelis, E. P. 1997. Polymer melt intercalation in organically-modified layered silicates: Model predictions and experiment. *Macromolecules* 30:8000-8009.
- Vaia, R. A., Tekolsky, R. K., and Giannelis, E. P. 1994. Interlayer structure and molecular environment of alkylammonium layered silicates. *Chem. Mater.* 6:1017-1022.
- Wang, H., Zeng, C., Elkovitch, M., Lee, L. J., and Koelling, K. W. 2001. Processing and properties of polymeric nano-composites. *Polym. Eng. Sci.* 41:2036-2046.
- Willett, J. L., Millard, M. M., and Jasberg, B. K. 1997. Extrusion of waxy maize starch: Melt rheology and molecular weight degradation of amylopectin. *Polymer* 38:5983-5989.
- Xu, Y., Zhou, J., and Hanna, M. A. 2005. Melt-intercalated starch acetate nanocomposite foams as affected by type of organoclay. *Cereal Chem.* 82:105-110.
- Yoon, P. J., Hunter, D. L., and Paul, D. R. 2003. Polycarbonate nanocomposites. 1. Effect of organoclay structure on morphology and properties. *Polymer* 44:5323-5339.
- Zhu, L., and Xanthos, M. 2004. Effects of process conditions and mixing protocols on structure of extruded polypropylene nanocomposites. *J. Appl. Polym. Sci.* 93:1891-1899.

[Received September 6, 2005. Accepted March 2, 2006.]